CANADIAN JOURNAL OF EXPLORATION GEOPHYSICS
VOL. 29, NO. 1 (JUNE 1993), P. 177-188

VELOCITY AND ATTENUATION ANISOTROPY CAUSED BY MICROCRACKS AND MACROFRACTURES IN A MULTIAZIMUTH REVERSE VSP

ENRU LIU[1], STUART CRAMPIN[1,2], JOHN H. QUEEN[3] AND WILLIAM D. RIZER[3]

ABSTRACT

Previous analyses of crosshole survey (CHS) and reverse vertical seismic profile (RVSP) data sets at the Conoco Borehole Test Facility (CBTF) have shown that fracture parameters can be estimated from seismic data. Continuing this development, we analyse data recorded from shear-wave sources in a shallow multiazimuthal RVSP. The RVSP data cover 160° of azimuth and display symmetry in arrival times and amplitudes about an azimuth of approximately N70°E. They can be interpreted as both velocity anisotropy (azimuthal variation of traveltimes) and attenuation anisotropy (azimuthal variation of amplitudes). Since the direction N70°E has been previously identified as the strike of the dominant macro- and microfractures, as well as the direction of maximum horizontal stress at depth in the area, the observed velocity and attenuation variations can be interpreted in terms of stress-aligned fractures and microcracks. The data also show evidence of scattering characteristic of large-scale fractures. These interpretations are confirmed by matching synthetic seismograms to the field data, where the observed symmetry features in the seismograms are well-reproduced in the synthetic data.

Nearby surface exposures suggest there are two approximately perpendicular fracture sets at CBTF. In such media, the polarizations of shear waves are expected to be complicated and we show that under appropriate circumstances it is possible to infer multiple fracture sets if sufficient azimuthal coverage is available in either VSPs or RVSPs. The shear-wave polarizations, when plotted in equal-area polar projections, show two maxima in directions which are approximately orthogonal and almost exactly parallel to the strikes of the two fracture sets at a neighbouring surface outcrop. The observed shear-wave polarizations are well-matched by the synthetic shear-wave seismograms calculated for media with two fracture sets. The remarkable agreement between measured shear-wave polarizations from RVSP data, CHS data and borehole data and from the synthetic seismograms confirms the usefulness of shear waves for mapping subsurface fractures.

INTRODUCTION

There is increasing interest in fracture characterizatior using geophysical methods, particularly shear-wave anisotropy and shear-wave splitting (reviewed by Crampin and Lovell, 199 1; Crampin, 1993). The Conoco Borehole Test Facility (CBTF) in Kay County, Oklahoma, is an excellent laboratory for the study of naturally fractured rock. Over the past few years CBTF has been the site of an extensive programme of integrated geological studies (surface mapping, core analysis and well-log analysis), geophysical studies [crosshole surveys (CHSs), vertical seismic profiles (VSPs) and reverse VSPs (RVSPs)] and hydrological studies (fluid flow measurements) conducted around an array of shallow groundwater boreholes about 50 m deep. Results from various studies have been reviewed by Queen et al. (1992). This paper is part of these integrated studies and is a continuation of our early analyses of CHS, VSP and RVSP data sets (Queen and Rizer, 1990; Queen et al., 1990; Rizer, 1990; Liu et al., 1991a, 1991b; Lines et al., 1992). The RVSP data analysed here provide convincing evidence of fracture-related seismic velocity anisotropy and attenuation anisotropy.

This paper makes three principal contributions. Firstly, it shows clear evidence of systematic azimuthal traveltime and amplitude variations due to fractures at shallow depths from a multiazimuthal RVSP at CBTF site. The data also show evidence of the scattering characteristic of intermediate-length fractures where the fracture length and spacing are of the same order as the seismic wavelength. The observed variations in traveltime and amplitude are indicative of fracture-related velocity and attenuation anisotropy and are modelled with synthetic seismograms, although the scattering thought to be caused by intermediate-length fractures has not yet been adequately modelled mathematically. Secondly, it illustrates the possibility of using multiazimuth VSPs or RVSPs to map both single and multiple subsurface fracture sets. The measured initial shear-wave polarizations show two clear directions which are almost parallel to the strikes of the two fracture sets mapped from surface outcrops. This result is further supported by a comparison with theoretical predictions. Thirdly, it shows that the results obtained from seismic

'British Geological Survey, Murchison House, West Mains Road, Edinburgh EH9 3LA
'Department of Geology and Geophysics, University of Edinburgh, West Mains Road, Edinburgh EH9 3JW
"Exploration Research and Services, Conoco Inc., P.O. Box 1267. Ponca City, Oklahoma 74603

We thank Conoco Inc. for providing the RVSP data sets. The necessary preprocessing (including the rotary source decomposition) of the data was performed at Conoco Inc., where J.B. Sinton, V.D. Cox and P.L. Buller performed most of the early analyses with J.H. Queen. We thank P. Wild and X.-W. Zeng for help with the data processing and D.C. Booth for useful discussion and comments. We also thank D. Corrigan and another anonymous reviewer for their comments for improving the manuscript. Synthetic seismograms were calculated using the ANISEIS package of Macroc Ltd. and Applied Geophysical Software Inc. This work was supported by Conoco (UK) Ltd. through Contract No. 2.343 and the Natural Environment Research Council and is published with the approval of Conoco Inc. and the Director of the British Geological Survey (NERC).

data can be well-correlated with geological and hydrological data and confirms the importance of shear-wave analysis for fracture characterization.

DATA ACQUISITION AND PREPROCESSING

Data sets from shallow (50 m) multiazimuthal RVSPs recorded at CBTF have been analysed previously in an attempt to estimate the fracture parameters by Liu et al. (199 la), which will be referred to as Paper 1. The site geology is well-documented by Queen and Rizer (1990) and Rizer (1990). The target formation for these studies is a 13 m-thick section of fractured Barneston Limestone (known locally as Fort Riley Limestone) at depths between approximately 16 and 29 m, sandwiched between impermeable shales (Queen and Rizer, 1990; Rizer, 1990). Geological and geophysical studies indicate the presence of nearly orthogonal subvertical fractures in the target formation consisting of a dominant N70°E fracture set interconnected by a secondary N20°W set visible on nearby outcrops in Figure la. This fracture pattern can be traced on outcrops in the Fort Riley Limestone Formation from about 5 km away to within a few hundred metres of the CBTF site. Figure lb shows the layer-cake velocity depth structure.

The RVSP surveys were carried out at borehole GW-3 with sources located at depths between 1.5 and 38.4 m with 0.6 m spacing. Figure lc and Table 1 show the source-receiver geometry. The recording was performed in two phases: two orthogonal lines of increasing offset (surface geophones Gl to G4 and G5 to G8) and an equally spaced 160" arc with offset of 7.6 m (geophones G9 to G16). Only data recorded on geophones on the arc around GW-3 (G2 and G9 to G 16) are analysed here.

Table 1. Azimuths and offsets of geophone positions for RVSPs in well GW-3, with source every 0.6 m from 1.5 m to 38 m depth.

Geophone Number	Geophone Azimuth (N°E)	Geophone Offset (m)
1	160.5	4.51
2*	160.5	7.62
3	160.5	10.72
4	160.5	13.78
5	65.5	4.51
6	65.5	7.62
7	65.5	10.51
8	65.5	13.51
9*	141.5	7.62
10*	123.5	7.62
11*	105.5	7.62
12'	87.5	7.62
13*	51.5	7.62
14*	33.5	7.62
15*	15.5	7.62
16*	-2.5	7.62

*geophone position on arc around well GW-3.

The Conoco borehole source is a rotating eccentric mass radiating horizontally polarized shear waves; a detailed description is given by Hardage (1992). The mass is rotated in clockwise and anticlockwise directions and the data are demultiplexed and sweep correlated before decomposition into linear equivalents of radial and transverse components (in-line and cross-line, respectively). The orientation of each correlation vector sweep is obtained from a compass attached to the source. The three-component traces are oriented as vertical (Z), radial (X) and transverse (Y) components. The current source has a frequency band of approximately 50 to 300 Hz and is recorded at a sampling rate of 1000 samples/s. A band-pass filter between 50 to 220 Hz removes noise outside the band of interest. The full-wave synthetic modelling in Paper 1 suggests that this source yields impulsive SH- and SV-wave signals for nearly vertical raypaths that can be modelled synthetically using horizontal forces. In this paper, we sought to analyse the shear-wave behaviour in data that were as close to being unprocessed as possible and no other processing apart from that described above was applied to the data.

DATA ANALYSIS AND EVIDENCE OF FRACTURES

Figure 2 shows examples of recorded RVSP data displayed in common-source gathers for the arc of ten surface geophones from source locations at the top (17.4 m), middle (23.5 m) and bottom (29.6 m) of the 13 m-thick Fort Riley Limestone layer. [The radial component of geophone G2 (azimuth N160.5°E) did not function.] The horizontal seismograms are displayed in four-component format, where rows are source and columns are geophone components for in-line (X) and cross-line (Y) orientations. All figures show true relative amplitudes unless specified otherwise, so that amplitudes between traces and between components may be directly compared. These figures display systematic amplitude and traveltime variations with azimuth, which are present on almost all common-source gathers for all source depths, except for 1) the two shallowest depths (1.5 and 2.1 m) which show relatively large scatter attributable to surface waves in the low-velocity near-surface layers and 2) those below the Fort Riley Limestone Formation. Both XX and YY components (X source recorded by X receiver and Y source recorded by Y receiver, respectively) show similar variations, and at some azimuths there is evidence of pronounced scattering in the coda following both *P*- and shear waves.

The seismograms show particularly strong scattering when the source is located below about 30 m, that is, below the large velocity contrast at the base of the Fort Riley Limestone layer. There is little evidence of systematic variation in velocity or amplitude at these depths. It is suggested that this scattering is the result of reverberations in the low-velocity layer below the limestone.

Fracture detection based on variations of traveltime and amplitude

The variation of shear-wave arrival times in Figure 2 shows approximate symmetry about the centre of displays. Figure 3a is a plot of these visually picked traveltimes

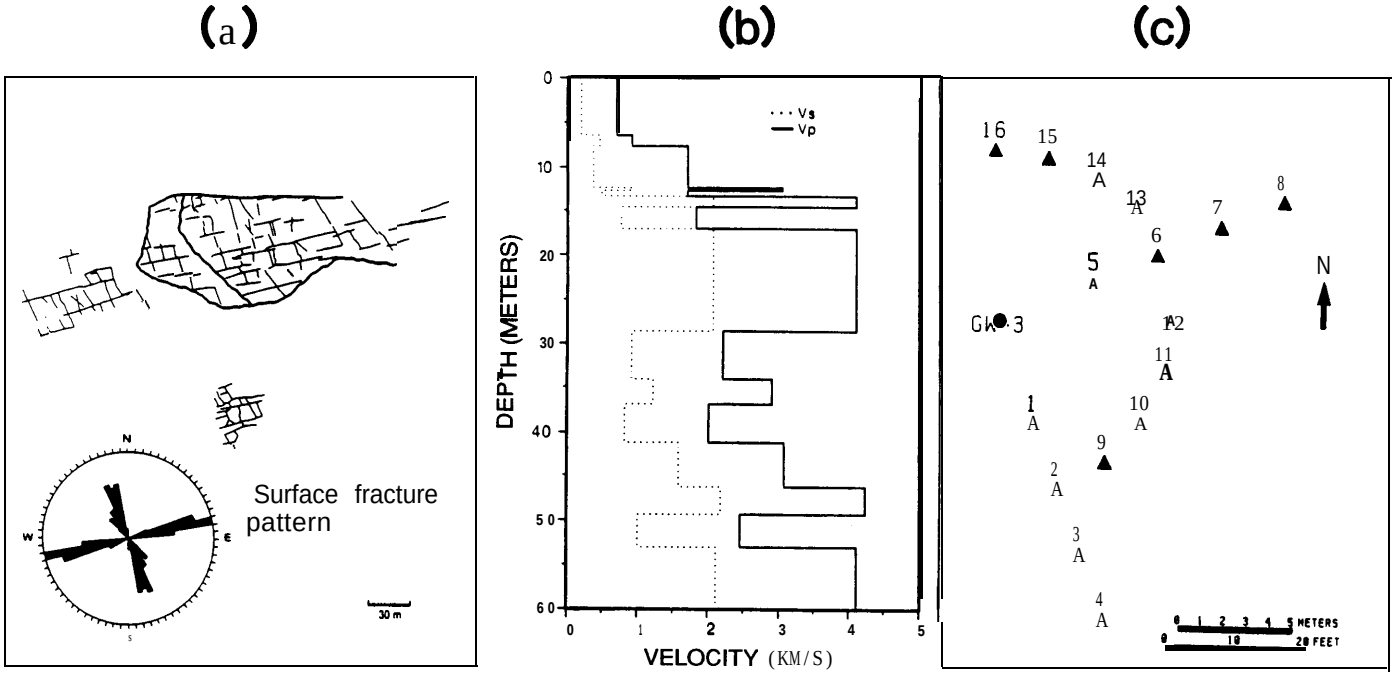

Fig. 1. (a) Map of surface fracture patterns at a nearby outcrop of Fort Riley Limestone and rose diagram of fracture orientations (after Queen and Rizer, 1990). (b) Shallow mean *P*- and S-wave velocity structure at Conoco Borehole Test Facility. (c) Recording geometry for RVSP experiments with rotary source in the well GW-3. The recording was in two phases, radial lines, geophones G1 to G4 and G5 to G18, and an azimuthal arc at offset of 7.6 m, G9 to G16.

against azimuth at fixed offset for the source at a depth of 23.5 m (Figure 2b). There is approximate symmetry about N90°E marked with a large arrowhead. This is in reasonable agreement (within 20") with the strike of the aligned cracks N70°E suggested in Paper 1 and with the regional stress-direction in Queen and Rizer (1990), and the symmetry in traveltimes can be attributed to fracture-related seismic velocity anisotropy. Similar symmetries can be seen in almost all common-source gathers as noted above.

Azimuthal variations begin to appear for source depths below about 3 m. Since the thickness of the uppermost layer is about 8 m and has a very low shear-wave velocity of about 200 m/s, the azimuthal variations suggest that this surface layer has pronounced anisotropy. This will be discussed in more detail in the next section.

There is also symmetry in the amplitudes of the shear-wave signals. Figure 3b shows the variation of amplitude with azimuth of offset for the seismograms in Figure 2b. The measurements are the amplitudes of the first cycle of shear waves normalised by the maximum amplitude. This is subjective, particularly when there is a low signal-to-noise ratio, but it does indicate the symmetry. The arrowhead indicates a low-amplitude symmetry direction of about N90°E. As with the traveltime variation in Figure 2, the amplitude of the shear waves is symmetric in a direction of about N90°E. This variation again suggests fracture-related attenuation anisotropy.

Both traveltimes and amplitudes show a symmetry about a direction N70°E to N90°E very close to the dominant fracture orientation of Figure 1 and the fracture orientation estimated from shear-wave polarization in Paper 1. As a check to the interpretation of these azimuthal variations in terms of fractures striking N70°E, which was obtained in Paper 1, the four-component seismograms have been rotated into the presumed fracture orientation of N70°E. Figure 4 shows the rotated seismograms of Figure 2b, where the off-diagonal energy has been reduced, so that it is difficult to distinguish noise and signals in the off-diagonal components, suggesting that the interpretation in terms of dominant fracture orientations is approximately correct.

Fracture detection based on waveform character

Another feature of the gathers is the character of the waveforms. This can be seen most clearly when each trace (in Figure 2a) is individually normalised (Figure 5). The waveforms with large shear-wave amplitudes in Figure 2 are relatively simple with low-amplitude coda. In contrast, where the amplitudes of the main shear-wave arrival are small in Figure 2 (for example, close to the direction of the dominant fractures), the coda of both P-waves and shear-wave arrivals in Figure 5 is more pronounced, particularly on the radial source and geophone components (the other gathers show similar phenomena). In these directions the seismic energy is scattered uniformly throughout the coda rather than being concentrated near the main shear-wave arrival as with other offset azimuths. This is the reason for the low amplitudes across the centre of the plots in Figure 2, where obvious shear-wave arrivals are sometimes absent

We suggest that this difference in character of the waveform results from interactions with the large-scale fractures known to exist at the study area in the target formation of Fort Riley Limestone (Paper 1; Queen and Rizer, 1990).

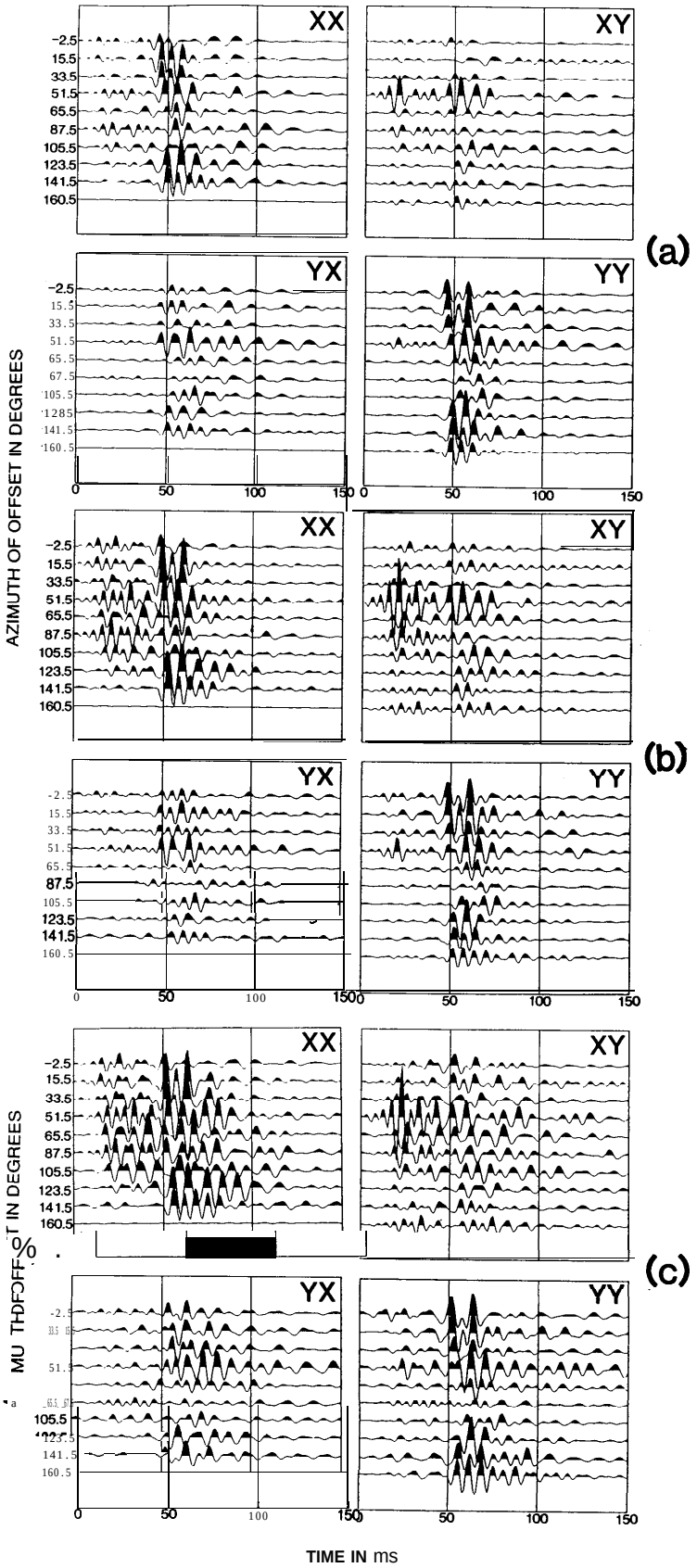

Fig. 2. Examples of RVSP data for common-source gathers displayed in four-component format for ten azimuths for source depths of: (a) 17.4 m; (b) 23.5 m; and (c) 29.6 m. Rows represent in-line (X) and cross-line (Y) source components and columns represent in-line (X) and cross-line (Y) geophones.

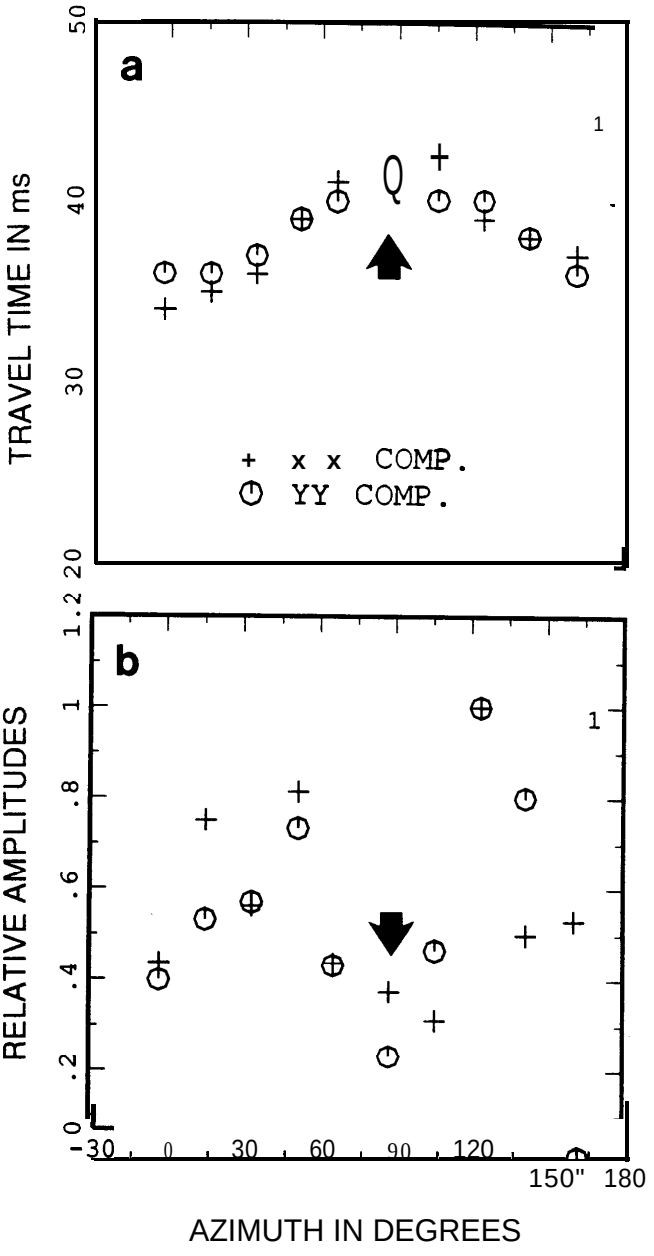

Fig. 3. Plots of visually-picked attributes against azimuth for observed XX- and YY-component common-source gathers for source at 23.5 m in Figure 2b: (a) traveltime; and (b) amplitude. Arrowheads indicate approximate symmetry directions.

Variations in traveltime and amplitudes are also observed for sources above the Fort Riley Limestone Formation, suggesting that strong anisotropy also exists in the near-surface shales. Our interpretation is that in the direction close to the strikes of fractures, most of the energy will be internally reflected at large angles of incidence when the fracture length and spacing are appropriate. At larger angles of incidence to the fracture face, as along other offset azimuths, more of the energy will be transmitted and the energy loss due to reflection and refraction is comparatively small.

If the lengths of the fractures are a substantiai fraction of the source-to-geophone distance, there are two possibilities. If there are several parallel fractures, the seismic energy will

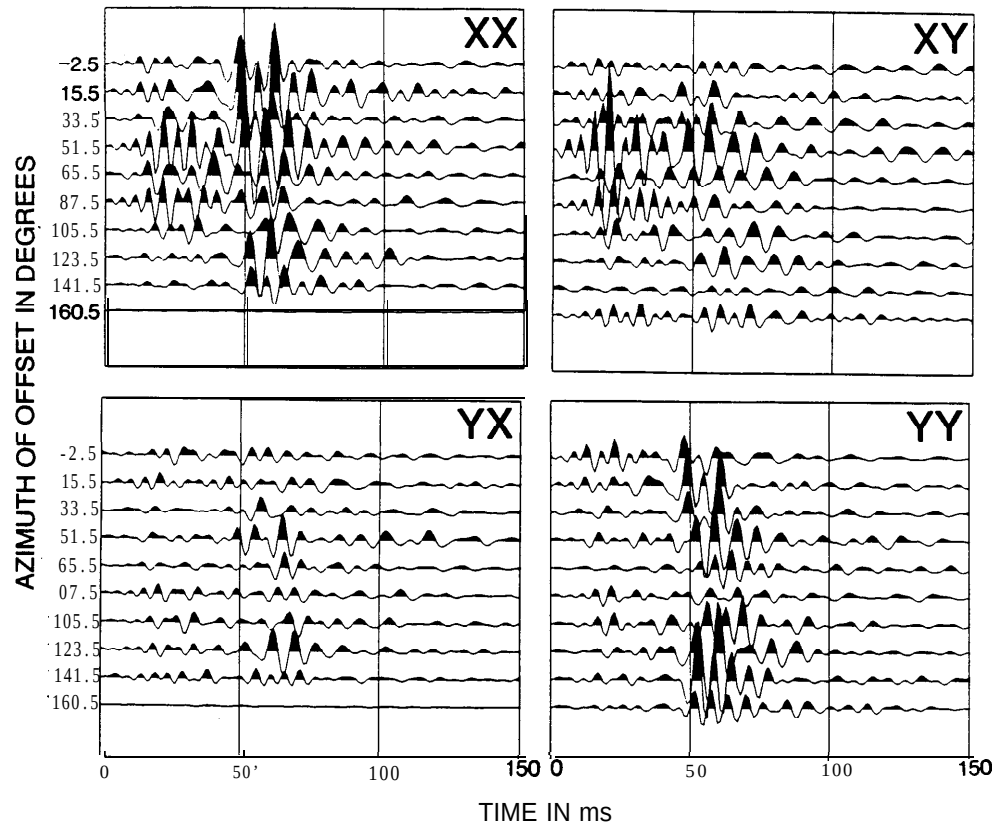

Fig. 4. Seismograms of Figure 2b rotated parallel (X) and perpendicular (Y) to the presumed fracture orientation of N70°E.

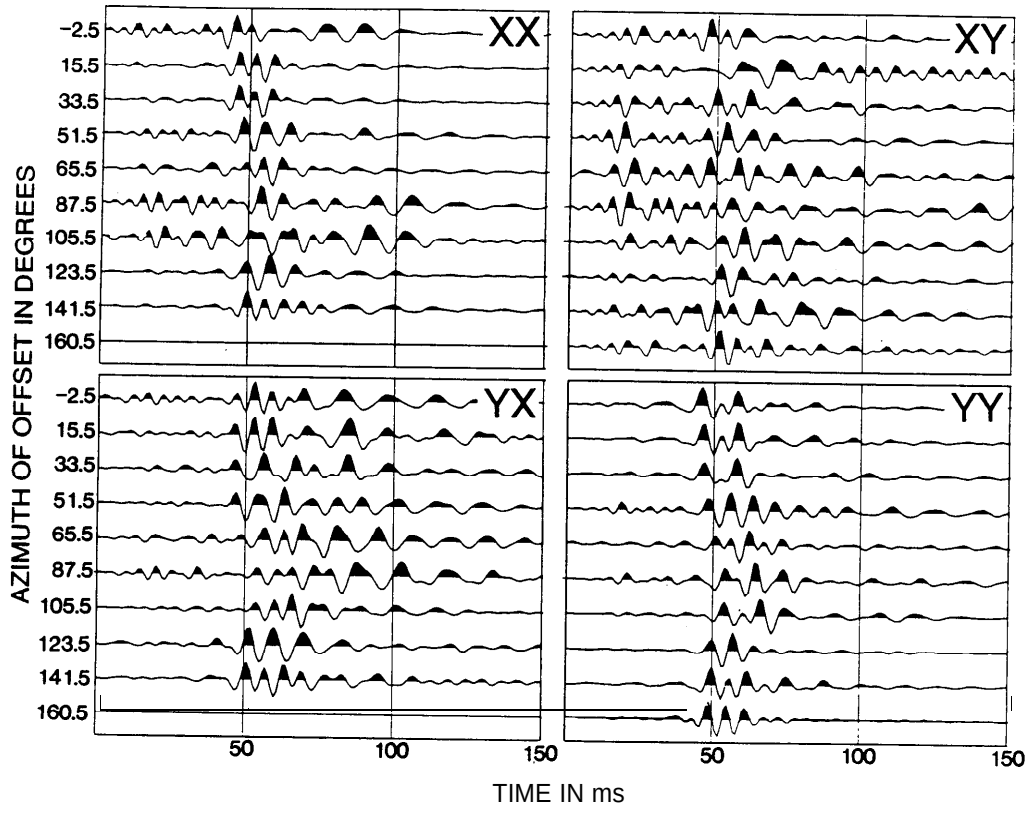

Fig. 5. Seismograms of Figure 2a but with four-component seismograms individually normalised.

be trapped and channel waves may be expected, when both source and geophone are located between parallel fractures. If there is a single large fracture on one side or other of well GW-3, asymmetry would be expected in the distribution of amplitude and possibly velocity either side of the fracture, such as the shadow zones reported by Fehler and Pearson (1984) and Niitsuma and Saito (199 1). Such asymmetry is not seen, and the data appear to display neither channel waves nor shadow zones, suggesting that more than one fracture exists with lengths shorter than the source-to-geophone distance. When the fracture length is much shorter than the seismic wavelengths (4 to 10 m), the resulting scatter might be expected to cause little attenuation. The seismograms in Figure 2 show substantial attenuation at azimuths between N70°E and N90°E. Since these various effects do not appear to be caused by fractures which are much longer or much shorter than the seismic wavelength, we suggest that the attenuation, velocity anisotropy and scattering is caused by intermediate-length fractures with dimensions similar to those of the seismic wavelengths of 4 to 10 m. To our knowledge, the effects of such intermediate-length fractures have not yet been modelled.

Fracture detection based on shear-wave polarization and evidence of biplanar fracture sets

In Paper 1, we analysed the RVSP data sets and estimated crack parameters from the polarizations of the faster split shear waves and the time delays between the split shear waves using two automated techniques: the linear-transform technique of Li and Crampin (1991) and the rotation technique of Alford (1986). These polarization results are now reproduced in Figure 6. Figure 6a shows histograms of the measured polarizations of the faster split shear waves over 5° intervals. There is a maximum near N70°E and a secondary maximum near N150°E. The estimated polarizations of the faster split shear waves shows a remarkable consistency and indicates a fracture orientation of approximately N70°E ± 10" corresponding to the symmetry axis identified in traveltimes and amplitudes in Figure 3.

Extensive studies reported by Queen and Rizer (1990) suggest that there are two nearly orthogonal sets of vertical parallel fractures within the Fort Riley Limestone Formation with a conjugate angle of about 80" (Figure 1). Two maxima in the histogram of Figure 6a are in the directions of these two fracture sets. In an integrated study of fracture patterns at CBTF, Queen and Rizer (1990) first suggested that it may be possible to infer subsurface fracture patterns using shear-wave polarization data from relatively deep azimuthal VSPs. Following this idea, a study of effects of biplanar fracture sets (and, by implication, of multiple fracture sets) was made by Liu et al. (1993), referred to as Paper 2. They show that when two or more sets of vertical parallel fractures are combined with a conjugate angle of less than about 50°, the average polarization of the faster split shear waves within the shear-wave window are in the direction of crack density weighted average of two fracture sets:

$$\phi_{eff} = (\varepsilon_1\phi_1 + \varepsilon_2\phi_2) / (\varepsilon_1 + \varepsilon_2), \quad (1)$$

where ε_1 and ε_2 are the crack densities and ϕ_1 and ϕ_2 the strikes of the two fracture sets, respectively, where $\varepsilon = Na^3/v$, and N is the number of cracks of radius a in volume I?. The effective crack density of the biplanar system is the sum of the crack densities of individual crack sets:

$$\varepsilon_{eff} = \varepsilon_1 + \varepsilon_2. \quad (2)$$

Equation (1) is a good first-order approximation for conjugate angle of less than or equal to about 50" and equation (2) is exact. However, if the conjugate angle is greater than 50°, two distinct polarization directions are apparent in the shear-wave window (Paper 2).

Figure 6b is an equal-area rose diagram of the histogram in Figure 6a. The dominant maximum is in the direction N70°E but there is a secondary maximum at about N 150°E (the dominant crack set from surface outcrops is marked with arrowheads). This compares very well with Figure 6c, which is the rose diagram for fractures induced in discs of Fort Riley Limestone from surface outcrops during Point Loading tests (after Queen and Rizer, 1990). This rose plot is interpreted as indicating the orientations of macrofractures mapped in the outcrops (Queen and and Rizer, 1990). There is remarkable similarity in the directions of the two maxima in Figures 6b and 6c. Following the techniques of Paper 2 for modelling biplanar sets of cracks, we construct a solid with two sets of vertical cracks with crack densities $\varepsilon_1 = 0.07$ and $\varepsilon_2 = 0.035$ with a conjugate angle of 80". (The sum of crack densities $\varepsilon = 0.105$ is similar to the crack density determined in Paper 1.) Figure 6d shows equal-area rose diagrams of the polarizations of the leading split shear waves within the shear-wave window of this solid. Again, two distinct directions can be seen with similar relative amplitudes, and the rose diagrams of shear-wave polarizations (Figure 6b), induced fracture patterns (Figure 6c) and theoretical biplanar solid (Figure 6d) are very similar.

MODELLING SYNTHETIC SEISMOGRAMS

We have shown various evidence for seismic anisotropy at CBTF and have suggested that fractures are the dominant cause of the observed variations in traveltime and amplitude. However, there are some difficulties in explaining the observed variations in terms of the current understanding of seismic wave propagation in cracked and fractured media. The main difficulty is that in the four-component seismograms of Figure 2 both XX and YY components show similar variations of arrival time and amplitude which are symmetrical about the direction of the strike of the dominant fracture set. There is expected to be a reciprocal relationship between velocity and attenuation in a cracked solid (Crampin, 1984), and although the symmetry of the YY components can be modelled, the similar variations of YY and XX components cannot both be modelled synthetically by a uniform distribution of cracks striking parallel to N70°E throughout the structure.

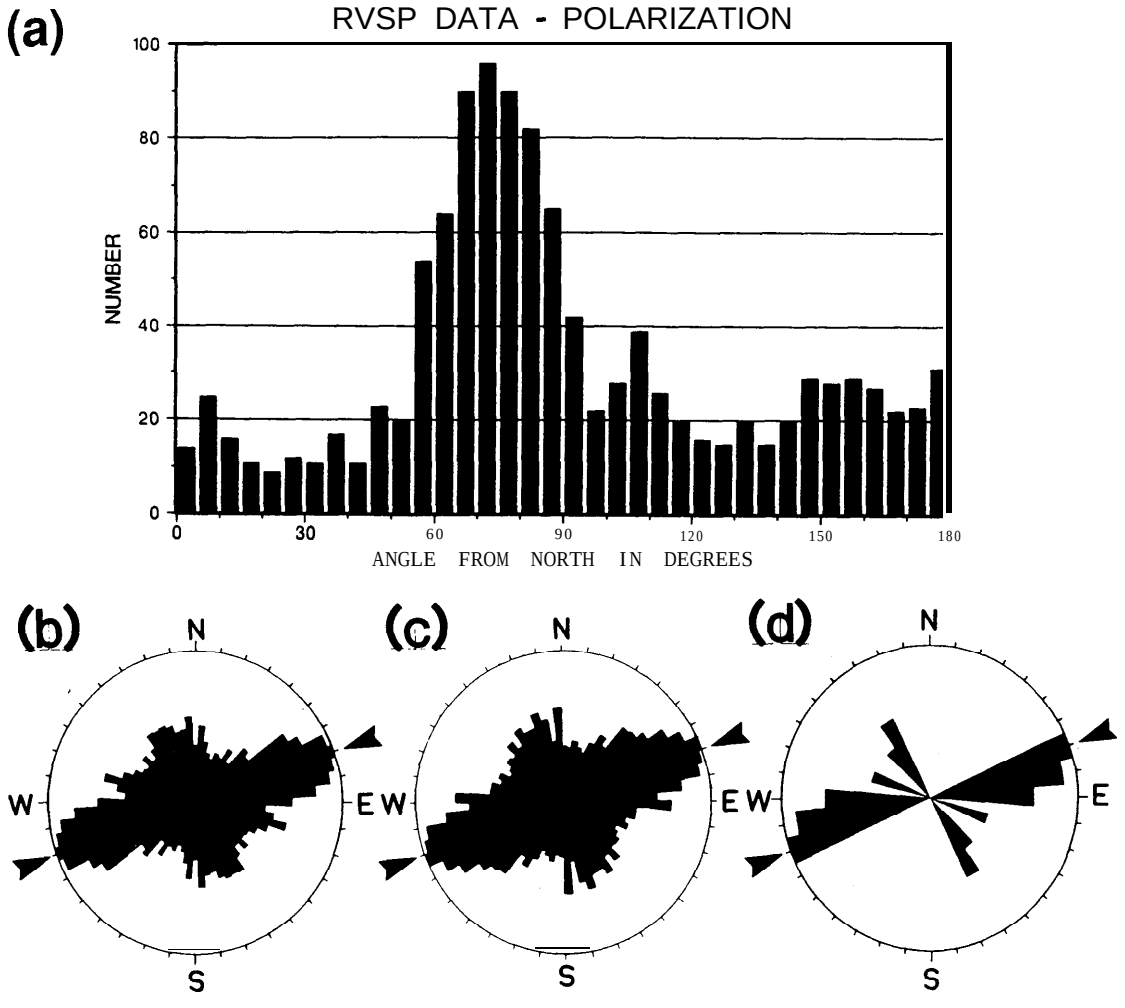

Fig. 6. (a) Histograms of the estimated polarization of shear-wave arrivals in the RVSP data (after Paper 1). Equal-area rose diagrams of: (b) shear-wave polarizations from (a); (c) normalized cumulative fracture length versus direction for the traces of fractures induced in Fort Riley Limestone samples (after Queen and Rizer, 1990); and (d) theoretical shear-wave polarizations within the shear-wave window of the proposed biplanar crack distribution. Arrowheads indicate the dominant fracture orientation.

Anisotropy of surface layer

The common-source gathers display very similar azimuthal variations of arrival time and amplitude for all source levels above and throughout the Fort Riley Limestone . . (except for the two uppermost levels of 1.5 and 2.1 m). This suggests that the surface layers may have a dominant effect on the azimuthal variations for surface recordings. The complications of shear waves and anisotropy in the near-surface layers has long been recognized and various causes have been identified. The rotation of the direction of minimum stress, which controls the orientation of fluid-filled inclusions, are sometimes found as the lithostatic stress decreases towards the surface (Crampin, 1990). Extremely low shear-wave velocity in near-surface layers can cause anomalous shear-wave arrivals (Campden et al., 1990), and there may be other factors [see the discussion of Natural Directivity in Slater et al. (1993)]. There has been no geological assessment of fracturing in the shales above the Fort Riley Limestone in the study area. This shale is decomposed into soil. The nature of deformation and failure of soil is complex and is poorly understood. In order to model both XX and YY components, we use distributions of cracks with coplanar-normals above the Fort Riley Limestone (crack faces randomly oriented and parallel to the direction of N70°E) and parallel vertical cracks in the Fort Riley Limestone Formation.

Figure 7a shows the variation of velocity and attenuation (l/Q) of body waves in a plane parallel to the crack face through a distribution of water-filled coplanar-normal cracks, with a crack density of $\varepsilon = 0.10$ and a crack radius of 4 m, in an isotropic, low-velocity rock simulating the crack-induced anisotropy of the surface layer at the CBTF site. Figure 7b shows similar variations in a plane through the crack normals in a distribution of parallel water-filled cracks with a crack density of $\varepsilon = 0.1$ in an isotropic rock simulating the crack-induced anisotropy of the Fort Riley Limestone Formation. The pattern of reciprocity of velocity and attenuation in Figure 7 is similar to that observed in Figure 3. Since the

formulations of Hudson (198 1) only model the attenuation caused by scattering, we use the- formulations schematically and attempt to model attenuations with the relatively large crack length of 4 m for both models in Figure 7, without any reference to the crack size in the real rock. The variations for coplanar-normal cracks in Figure 7a show little velocity anisotropy but substantial attenuation anisotropy, as might be expected when the shear-wave velocity is very small (about 200 m/s). This suggests that even when the velocity anisotropy is small there may still be a strong attenuation anisotropy.

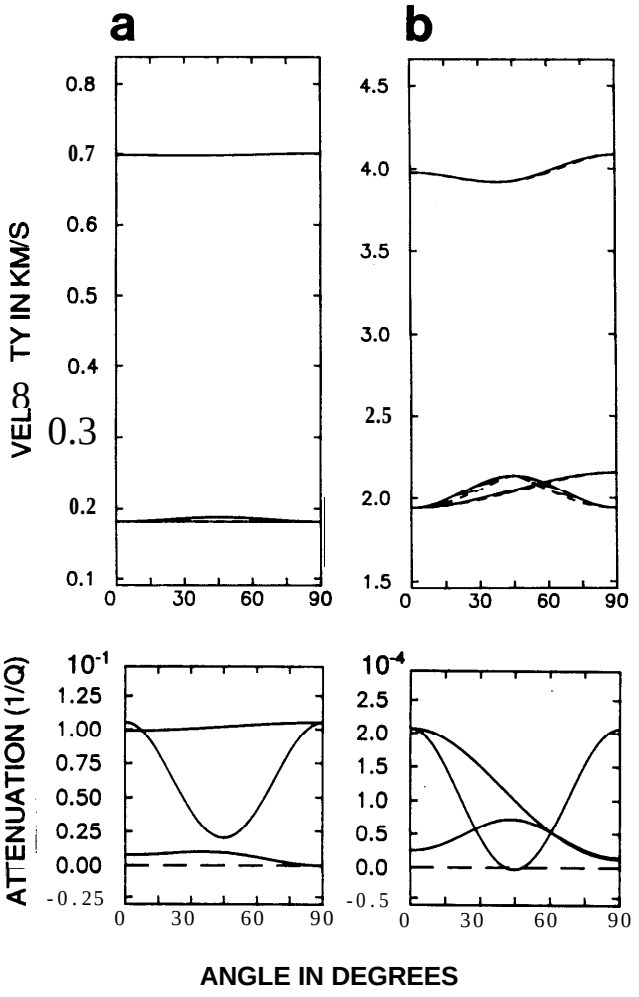

Fig. 7. **(a)** Variations of velocity and attenuation in a plane parallel to the crack face in a distribution of thin water-filled cracks with coplanar normals and crack density $\varepsilon = 0.1$ and radius 4 m in an isotropic low-velocity rock ($a = 700$ m/s, $\beta = 200$ m/s, $\rho = 2.0$ gm/cm^3) simulating the crack-induced anisotropy of the surface layer at CBTF. (b) Similar variations in a plane parallel to the crack normals in a distribution of parallel water-filled cracks with crack density $\varepsilon = 0.1$ in an isotropic rock ($a = 4100$ m/s, $\beta = 2200$ m/s, $\rho = 2.42$ gm/cm^3) simulating the crack-induced anisotropy of the Fort Riley Limestone. Solid lines are phase velocity and dashed lines in (b) are group velocity joined to phase velocity every 10° of phase-velocity direction.

Modelling observations with synthetic seismograms

We present synthetic full-wave seismograms as a final check of our interpretation of the RVSP data from CBTF. In Paper 1 we modelled cross-hole data and in Liu et al. (1991 b) we modelled the VSP data. Here, we calculate synthetic seismograms for the RVSP geometry based on these previous models and the velocity and attenuation variation of the surface layer and Fort Riley Limestone layer shown in Figure 7. Anisotropic attenuation is introduced using complex elastic constants (Crampin, 198 1, 1984). Background isotropic attenuation was also introduced, as in Paper 1. Figure 8a shows synthetic seismograms for the source depth of 23.5 m, corresponding to the observations in Figure 2b. Comparing the synthetic seismograms in Figure 8 with the observed seismograms in Figure 2b, the synthetic seismograms are in good agreement with the observations to the first order. The symmetry features in traveltime and amplitudes discussed above are well-matched. The principal difference is that the scattered wave fields across the centre of the plots in the observations are not reproduced in the synthetic seismograms.

Figure 8b shows the four-component seismograms of Figure 8a with the geophone axes rotated parallel and orthogonal to the N70°E strike of the cracks. Off-diagonal energy is significantly reduced, which again is in a good agreement with the observed seismograms in Figure 4. This suggests that although the RVSP data are significantly complicated by the effects of the near-surface layers, the observed and modelled velocity and shear-wave splitting are still primarily due to the fracture systems in the Fort Riley Limestone layer, although the attenuation is dominanted by the surface layers (Figure 7a).

DISCUSSION

A number of studies have shown lateral variations of shear-wave amplitudes in rotated records that can be attributed to the lateral variation of fracture intensity (Lewis et al., 199 1; Mueller, 199 1; amongst others, including several in this issue: Li et al., 1993; Yardley and Crampin, 1993; and others). However, these CBTF observations are amongst the first to display azimuthal variations of arrival times caused by aligned cracks, and almost certainly the first to display variations of attenuation caused by aligned cracks. As with most observations of seismic anisotropy, it is difficult to isolate the effects of anisotropy from other factors, which in this case include systematic geophone coupling, or miscoupling, the effects of the rotary source, inhomogeneity and, in particular, source radiation patterns in anisotropic solids. Inhomogeneities near the recording sites may cause scattering. It is unlikely that this could produce a strong alignment of polarizations and different sites would be expected to show different anomalies (irregularities). This makes it difficult to identify the effects of anisotropy if observations from only one point are available. Only when similar anomalies can be observed at several neighbouring

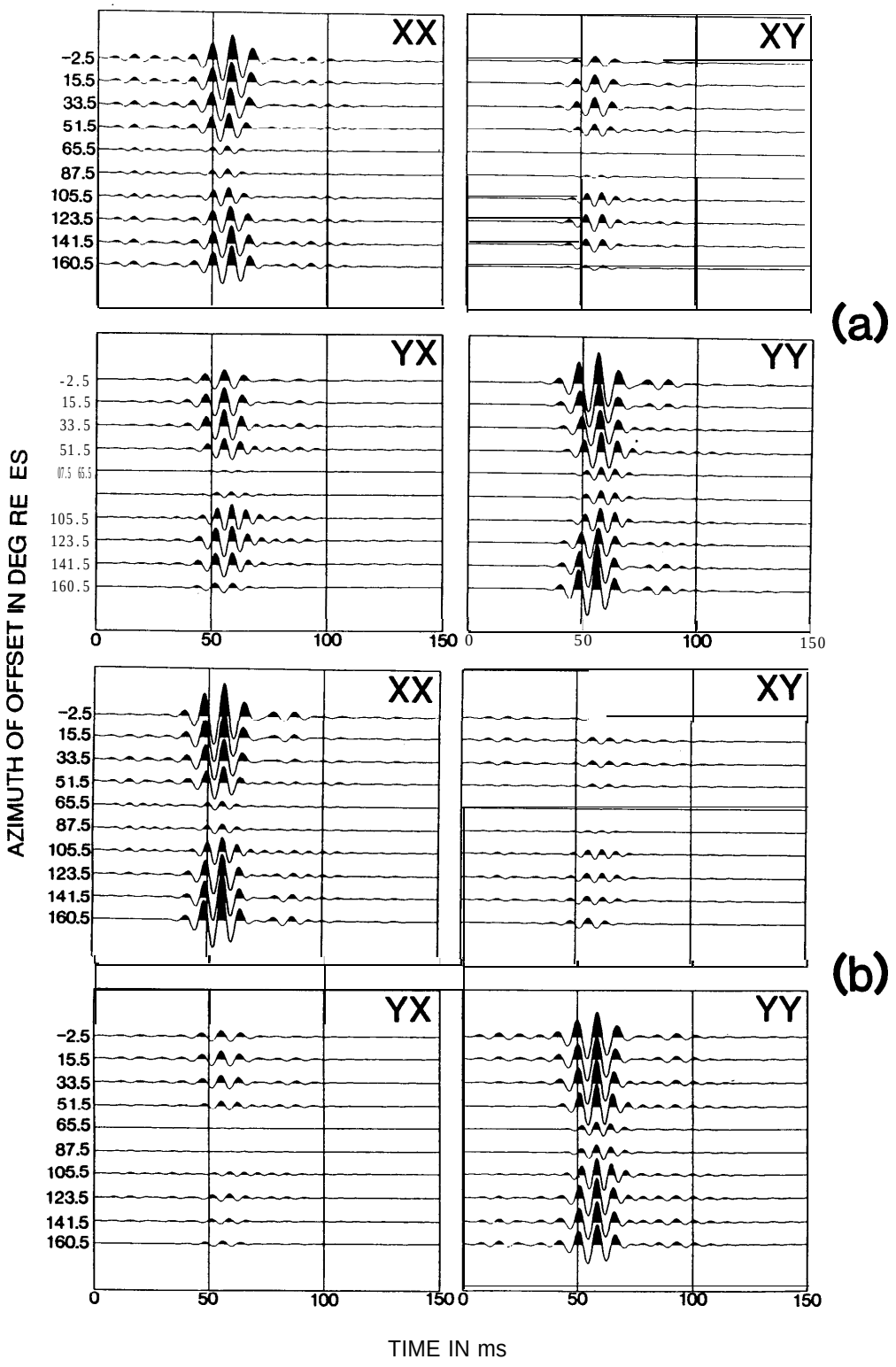

Fig. 8. Synthetic seismograms for the vertical fracture models aligned parallel to N70°E in the surface layer and striking parallel to N70°E in the underlying Fort Riley Limestones, where the variations of velocity and attenuation are given in Figure 7. (a) Geophone components in-line and cross-line; and (b) geophone components rotated parallel and perpendicular to the fracture orientation of N70°E.

recording sites is it possible to identify positively the presence of anisotropy along the travel paths. Since aligned polarization is observed along most of the azimuths (travel paths), it is unlikely that inhomogeneities are the dominant cause of the observations.

The results of this paper and Paper 1 correlate very well with other results and are consistent with other studies at CBTF, cited in the Introduction; thus we suggest that the models we present are a good first-order approximation to the real structure. Fracture-related seismic anisotropy is clearly present at CBTF causing anomalies in shear-wave traveltime, amplitude and polarization. The fracture systems obtained in this study correlate very well with other studies, including results from geological and hydrological data (Queen and Rizer, 1990; Rizer, 1990). The comparatively successful and detailed match of synthetic to observed seismograms for a plausibly realistic model in this paper gives us some confidence that we are analysing real geophysical effects with appropriate analytical and modelling techniques.

Possible fracture patterns at CBTF

Preliminary hydrological testing carried out in these shallow wells indicates excellent communication of fluid flow between GW-5 and GW-2 at an azimuth of N75°E and poor communication between GW-5 and three other wells, including GW-3 which is along the azimuth of about N95°E to GW-5 (Rizer, 1990). This indicates that the fluid flow is significantly along the dominant fracture direction. The simplest explanation for these high and low permeabilities is that there is a large fracture between GW-5 and GW-2 which does not intersect GW-3. The assumption of a single open fracture intersecting boreholes is not new. Beydoun et al. (1985) have successfuly used P-wave VSPs to detect such open (horizontal) fractures by analyzing fracture-generated tube waves. If such a fracture exists between GW-5 and GW-2, it must be nearer vertical than horizontal, since the isolated well GW-3 is less than 10” in azimuth from the direct line between GW-5 and GW-2.

If there were such a fracture, it might be expected that the amplitudes of waves transmitted across the fracture would be significantly reduced (Fehler and Pearson, 1984), and we might expect a shadow zone in the RVSP experiment (as found by Niitsuma and Saito, 1991) around well GW-3. Geophones located on opposite sides of the fracture from GW-3 (e.g., geophones 13, 14, 15 and 16), and these geophones located on the same side (geophones 2, 9, 10, 11 and 12) might be expected to show signals scattered by the fracture or, at least, the amplitudes would not be symmetrical on either side of the fracture. However, the RVSP presented here with the source in GW-3 shows a remarkable symmetry about the direction of N80°E, the direction between GW-5 and GW-2, suggesting that there is no single large open fracture between GW-5 and GW-2 passing close to GW-3.

The model used to explain the preferred fluid flow between GW-5 and GW-2 by Rizer (1990) is a network of biplanar cracks in the Fort Riley Limestone layer. Such fracture systems are very common in near-surface rocks (Lorenz et al., 1991). The dominant set is aligned approximately in the direction of the two wells GW-5 and GW-2 (N75°E) with the nearly orthogonal secondary set generally terminating against the dominant fracture set (Figure la). An explanation for the pattern of fluid flow of Rizer (1990) is that GW-5 and GW-2 are connected by such biplanar crack sets but GW-3 is within an intact block without large fractures. Paper 2 examined the behaviour of shear waves in media with biplanar cracks and showed that if the crack density of the secondary crack set is small compared with the dominant crack set (e.g., less than half), the behaviour of shear-wave polarizations and time delays between two split shear waves will be similar to monoplanar (parallel) cracks. The biplanar fracture model can thus in theory explain the preferred fluid flow between GW-5 and GW-2, the polarization alignment (Figure 6a) and symmetry features that we have shown in this paper (Figure 3).

Multiple fracture sets

We have demonstrated in Figure 6 that in some circumstances it is possible to map multiple fracture orientations using multiazimuthal VSPs and reverse VSPs. Multiple fracture sets are important because they would form a network and provide possible paths of fluid flow, which could explain the preferential fluid flow between well GW-5 and GW-2. In an extensive study with a variety of techniques, Queen and Rizer (1990) were able to map subsurface fracture patterns in some detail. Similarly, Wang and Sun (1990) and Blenkinsop (1990) were able to map the fracture patterns at Cajon Pass Drill Hole, California. In all of these studies, it was found that more than one fracture set existed with the one parallel to the maximum compressional stress dominant. Some conclusions of a study of seismic effects of multiple fracture sets made by Paper 2 have been summarised in this paper (equations 1 and 2). If such fracture systems are common, they provide channels for fluid flow and may have important implications for the hydrological investigations at shallow depths.

Microcracks and macrofractures

Up to now, most fracture studies have been concerned with the effects of microcracks on wave propagation. In Paper 1 and in this paper we have used effective elastic-constant microcrack models to calculate the synthetic seismograms and a reasonably good match between observations and synthetics has been achieved. From this point of view, it is reasonable to say that the microcrack model is a good approximation to the more complicated natural reservoir fracture systems as at CBTF. However, reservoir engineering is interested in larger fractures, where the length is of order of metres rather than millimetres or microns. This study suggests that the seismic response of large and small fractures may be similar and that the main difference is probably in the level of attenuation and waveform characteristics such as scattering, and that by analysing the variation, level of attenuation and waveforms of shear-wave seismograms it may be possible to estimate the dimension or size of the fractures.

Several formulations are available to study the response of seismic waves in media with microcracks. The most comprehensive are probably those developed in a series of papers by Hudson, beginning with Hudson (1980, 1981), where the cracked media are replaced with effective media with the same variation in elastic properties. The effect of attenuation can be modelled by complex elastic constants. Similarly, in media with infinite fracture length where the fracture spacing is much smaller than the seismic wavelength, the media can also be replaced with effective media in the first order (Schoenberg and Douma, 1988). The Schoenberg and Douma formulations are indistinguishable from those of Hudson if appropriate values of the variations of the normal and tangentional stiffnesses across the fractures are selected.

The results here suggest that when the fracture length and spacing are similar to seismic wavelengths scattering is important, particularly for shear waves with polarizations parallel to the crack face, and it is doubtful if an effective medium theory could be wholly appropriate for such intermediate-length fractures. This study also suggests that although the seismic waveforms may be complicated, shear-wave polarizations are still relatively stable and the direction of faster split shear waves are parallel to the strike of fractures. It appears that effective medium theory for microcracks may still give a good first-order match to the initial seismic response to intermediate-length fractures.

Recordings of shear-wave splitting are necessarily controlled by the anisotropic symmetry of the medium surrounding the geophone, and this is likely to vary rapidly near the surface and be sensitive to the effects of low-velocity weathered layers. Consequently, the quality of the symmetry displayed by the four-component seismograms is surprising, as is the match of synthetic to observed seismograms for plausible distributions of cracks. The models are not strictly unique, but nevertheless place reasonably tight constraints on possible crack distributions at the CBTF site.

CONCLUSIONS

1. The azimuthal RVSPs examined here are amongst the first data sets to display directly velocity and attenuation anisotropy due to aligned fractures.
   The velocity and attenuation of four-component seismograms can be matched to the first order by synthetic seismograms using a full-wave modelling package assuming an effective-medium long-wavelength model of aligned cracks.
2. The four-component seismograms display scattering when the polarizations of the shear waves are parallel to the crack face; the scattering is not modelled by the synthetic seismograms.
4. Although subsurface fracture patterns may be complicated, under certain circumstances it is possible to map subsurface multiple fracture sets using multiazimuthal VSPs or RVSPs. This may have important implications for shallow hydrological applications.
5. It has been well-established elsewhere that the seismic response to distributions of small fractures can be modelled by appropriate effective-medium formulations. It is suggested that these formulations still give a good first-order approximation to the response of seismic velocities, polarizations and possible attenuation to distributions of aligned intermediate-length fractures, when cracks have dimensions and separations of the order of the seismic wavelength. However, the scatter of the waveforms through such cracks cannot be modelled by effective-medium theory and more accurate general methods need to be developed.

REFERENCES

Alford, R.M., 1986, Shear data in the presence of azimuthal anisotropy: Dilley, Texas: 56th Ann. Intemat. Mtg., Soc. Expl. Geophys., Exp. Abstr., 476-479.

Beydoun, W.B., Cheng, C.H. and Toksöz, M.N., 1985, Detection of open fractures with vertical seismic profiling: J. Geophys. Res. **90**, 4557-4566.

Blenkinsop, T.G., 1990, Correlation of paleotectonic fracture and microfracture orientations in cores with seismic anisotropy at Cajon Pass Drill Hole: J. Geophys. Res. 95, 11,143-l 1,150.

Campden, D.A., Crampin, S., Majer, E.L. and McEvilly, T.V., 1990, Modelling the Geysers VSP: a progress report: The Leading Edge 9, 8, 36-39.

Crampin, S., 1981, A review of wave motion in anisotropic and cracked elastic-media: Wave Motion **3**, 343-391.

1984, Effective anisotropic elastic-constants for wave propagation through cracked solids: Geophys. J. Roy. Astr. Soc. 76, 135-145.

_____, 1990, Alignment of near-surface inclusions and appropriate crack geometries for geothermal hot-dry-rock experiments: Geophys. Prosp. 38, 621-631.

_____, 1993, Arguments for EDA: Can. J. Expl. Geophys. 29, 18-30.

_____ and Lovell, J.H., 1991, A decade of shear-wave splitting in the Earth's crust: what does it mean? what use can we make of it? and what should we do next?: Geophys. J. Intemat. **107**, 387-407.

Fehler, M. and Pearson, C., 1984, Cross-hole seismic surveys: application for studying subsurface fracture systems at a hot dry rock geothermal site: Geophysics **49**, 37-45.

Hardage, B.A., 1992, Crosswell seismology and reverse VSP: Geophysical Press, London.

Hudson, J.A., 1980, Overall properties of a cracked solid: Math. Proc. Cambr. Phil. Soc. 88, 371-384.

_____, 1981, Wave speeds and attenuation of elastic waves in material containing cracks: Geophys. J. Roy. Astr. Soc. 64, 133-150.

Lewis, C., Davis, T.L. and Vuillermoz, C., 1991, Three-dimensional multicomponent imaging of reservoir heterogeneity, Silo Field, Wyoming: Geophysics **56**, 2048-2056.

Li, X.-Y. and Crampin, S., 1991, Linear-transform techniques for analysing shear-wave splitting in four-component seismic data: 61st Ann. Intemat. Mtg., Soc. Expl. Geophys., Exp. Abstr., 5 l-54.

_____, Mueller, M.C. and Crampin, S., 1993, Case studies of shear-wave splitting in reflection surveys in South Texas: Can. J. Expl. Geophys. 29, 189-215.

Lines, L.R., Kelly, R.K. and Queen, J.H., 1992, Channel waves in cross-borehole data: Geophysics **57**, 334-342.

Liu, E., Crampin, S. and Queen, J.H., 1991a, Fracture detection using cross-hole surveys and reverse vertical seismic profiles at the Conoco Borehole Test Facility, Oklahoma: Geophys. J. Intemat. **107**, 449-463.

_____, _____ and - - - , 1991b, Estimating near-surface fracture systems from seismic anisotropy using combination of crosshole surveys, VSPs and reverse VSPs: 61st Ann. Intemat. Mtg., Soc. Expl. Geophys., Exp. Abstr., 103-106.

_____, _____, _____ and Rizer, W.D., 1993, Behaviour of shear-waves in rocks with two sets of parallel cracks: Geophys. J. Intemat. 113, 509-517.

Lorenz, J.C., Teufel, L.W. and Warpinski, N.R., 1991, Regional fractures I: mechanism for the formation of regional fractures at depth in flat-lying reservoirs: Bull. Am. Assn. Petr. Geol. 75, 1714-1737.

Mueller, M.C., 1991, Prediction of lateral variability in fracture intensity using multicomponent shear-wave surface seismic as a precursor to horizontal drilling in the Austin Chalk: Geophys. J. Intemat. **107**, 409-415.

Niitsuma, H. and Saito, H., 1991, Evaluation of the three-dimensional configuration of a subsurface articial fracture by the triaxial shear shadow method: Geophysics **56**, 2 118-2 128.

Queen, J.H. and Rizer, W.D., 1990, An integrated study of seismic anisotropy and the natural fracture system at the Conoco Borehole Test Facility, Kay County, Oklahoma: J. Geophy. Res. 95, 11,255- 11,273.

_____, _____, Liu, E., Crampin, S. and Lines, L.R., 1992, A review of research with a downhole source at the Conoco Borehole Test Facility: Presented at the Spring Symp. on Cross-borehole Geophysics, Geophys. Soc. Tulsa.

_____, Sinton, J.B., Cox, V.D. and Buller, P.L., 1990, Seismic detection of natural fractures in the near-surface - Part II: RVSP response: Presented at the 4th Intemat. Workshop on Seismic Anisotropy, July 2-6, Edinburgh.

Rizer, W.D., 1990, Seismic detection of natural fractures in the near-surface, Part I: site geology of the Conoco Borehole Test Facility: Presented at the 4th Intemat. Workshop on Seismic Anisotropy, July 2-6, Edinburgh.

Schoenberg, M. and Douma, J., 1988, Elastic wave propagation in media with parallel fractures and aligned cracks: Geophys. Prosp. **36**, 57 l-590.

Slater, C., Crampin, S., Brodov, L.Y. and Kuznetsov, V.M., 1993, Observations of anisotropic cusps in transversely isotropic clay: Can. J. Expl. Geophys. **29**, 2 16-226.

Wang, C.Y. and Sun, Y., 1990, Oriented microfractures in Cajon Pass drill cores: stress field near the San Andreas Fault: J. Geophys. Res. 95, 11,135-l 1,142.

Yardley, G.S. and Crampin, S., 1993, Shear-wave anisotropy in the Austin Chalk, Texas, from multioffset VSP data: case studies: Can. J. Expl. Geophys. 29, 163- 176.